

# Fabrication and characterization of neat and aluminium-doped titanium (IV) oxide fibers prepared by combined sol–gel and electrospinning techniques

Jerawut Kaewsane<sup>a</sup>, Pinpan Visal-athaphand<sup>a</sup>, Pitt Supaphol<sup>b</sup>, Varong Pavarajarn<sup>c,\*</sup>

<sup>a</sup> Department of Physics, Faculty of Science, King Mongkut's University of Technology Thonburi, Bangkok 10140, Thailand

<sup>b</sup> The Petroleum and Petrochemical College and The Center for Petroleum, Petrochemical and Advanced Materials, Chulalongkorn University, Bangkok 10330, Thailand

<sup>c</sup> Department of Chemical Engineering, Faculty of Engineering, Chulalongkorn University, Bangkok 10330, Thailand

Received 6 October 2009; received in revised form 29 March 2010; accepted 28 April 2010

Available online 23 June 2010

## Abstract

Sol–gel and electrospinning techniques were incorporated to produce polyvinylpyrrolidone (PVP)/titanium (IV) oxide composite fibers from solutions containing PVP and titanium tetraisopropoxide, with or without aluminium nitrate as the source of aluminium dopant. Upon the calcination of the as-spun fibers, the neat and the aluminium-doped titania fibers were obtained. Increasing the calcination temperature resulted in the decrease in the fraction of anatase phase within the fibers, as well as the increase in titania crystallite sizes. The presence of aluminium dopant, however, was found to greatly affect both physical and chemical properties of the synthesized titania fibers. Aluminium nitrate accelerated condensation of titanium oxide species during the sol–gel process, which resulted in increased viscosity of the spinning solution and consequently affected the diameters of the as-spun fibers. Aluminium dopant also played the major roles in both regulating the nucleation rate during crystallization of titania and controlling the growth mechanism of titania crystallites. As a result, the aluminium dopant caused the crystallite size of titania to decrease and retarded phase transformation from anatase to rutile.

© 2010 Elsevier Ltd and Techna Group S.r.l. All rights reserved.

**Keywords:** Titania; Nanofibers; Electrospinning; Doping

## 1. Introduction

Titanium (IV) oxide or titania ( $\text{TiO}_2$ ) is one of the most common materials for a variety of applications such as catalytic devices, sensors, solar cells, and other optoelectronic device [1,2]. Titania is a wide bandgap semiconductor with many interesting properties, such as transparency to visible light, high refractive index and low absorption coefficient. Other than these properties, it has been known to be an excellent photo-catalyst for the decomposition of various organic substances that include certain pesticides [3]. This pertains titania as excellent candidate for the treatment of agricultural waste water [4]. Titania is known to have three natural polymorphs, i.e., rutile, anatase, and brookite. Only anatase is generally accepted to have significant photocatalytic activity.

Titania can be synthesized by various techniques, such as precipitation [5], chemical vapor deposition [6], hydrothermal method [7], and glycothermal method [8]. Another common technique that can result in titania with an extremely high surface area is sol–gel method [9]. In the present work, the sol–gel method was combined with the electrostatic spinning or electrospinning technique in order to produce titania fibers.

Electrospinning technique is a facile method for fabricating ultrafine fibers with diameters ranging from tens of nanometers to less than ten micrometers. In a typical process, a stream of a polymer liquid (i.e., solution or melt) is ejected from a small capillary opening or a nozzle under the influence of a strong electric field. The build-up of charges on the surface of a droplet is responsible for the formation of the charged stream or a jet, which is subsequently stretched to form a continuous ultrathin fiber. During its flight to a collective target, the ejected charged jet dries out (for the solution) or cools down (for the melt), leaving ultrathin fibers in the form of a non-woven fiber mat on the target. The fiber mat has a high surface area-to-mass ratio with relatively small pore sizes [1,2,10]. Amorphous titania

\* Corresponding author. Tel.: +66 2 218 6890; fax: +66 2 218 6877.

E-mail address: [Varong.P@eng.chula.ac.th](mailto:Varong.P@eng.chula.ac.th) (V. Pavarajarn).

fibers have been reported to be successfully prepared from the electrospinning of a mixture of titanium tetraisopropoxide (TTIP), acetic acid, and a high molecular weight polyvinylpyrrolidone (PVP) [1].

Anatase is an unstable polymorph of titania. The transformation of anatase to rutile, which is the less chemically active polymorph, takes place at temperatures as low as 300 °C. Notwithstanding, the anatase-to-rutile transition temperature depends strongly on how titania is synthesized [11]. Titania is considered thermally stable if its anatase-to-rutile transformation temperature is relatively high. In catalytic applications, the titania structure that possesses a high surface area per unit mass with reasonably good thermal stability is desirable. As a consequence, a good number of studies have been devoted to improving the thermal stability, phase composition and pore structure of titania structures via the uses of metal dopants that include silicon [8] and aluminium [12,13]. Furthermore, it has been reported that the addition of certain metal dopants results in the enhancement of the photocatalytic activity of the resulting titania structures [9,14].

The main objectives of the present work are to investigate the effects of solution and calcination conditions on morphological appearance and crystal structure of the resulting titania fibers. The effects of the addition of aluminium as the secondary metal dopant on thermal stability and optical property of the resulting titania fibers were also investigated.

## 2. Experimental details

In a typical procedure, 1.5 g of titanium tetraisopropoxide (TTIP) was mixed with 3 mL of acetic acid and 3 mL of ethanol. The solution was allowed to rest for 10 min before being added into 7.5 mL of a 10 wt.% polyvinylpyrrolidone (PVP, Mw  $\approx$  1,300,000 Da) solution in ethanol. The mixture was constantly stirred for 10 min. The obtained solution was hereafter referred to as the neat spinning solution. Aluminium nitrate nonahydrate ( $\text{Al}(\text{NO}_3)_3 \cdot 9\text{H}_2\text{O}$ ) was finally added to the neat spinning solution at 0.1, 0.3 or 0.5 wt.% (based on the total mass of the final mixture) and the resulting mixtures were constantly stirred for another hour. These mixtures were hereafter referred to as the aluminium nitrate-doped spinning solutions. It should be noted that the spinning solution with the concentration of aluminium nitrate nonahydrate higher than 0.5 wt.% was too viscous to be electrospun into fibers.

Each of the spinning solutions was immediately loaded into a plastic syringe. A blunt 20-gauge stainless-steel hypodermic needle was used as a nozzle. The emitting electrode from a Gamma High Voltage Research ES30P power supply, capable of generation DC voltages up to 30 kV, was attached to the needle. The grounding electrode from the same power supply was attached to a piece of aluminium foil which was used as the collector plate, placed approximately 7 cm below the tip of the needle. Upon the application of a high voltage of 16 kV across the needle and the collective plate, a fluid jet was ejected from the nozzle. The flow rate of the spinning solution was 0.1 mL/min. As the jet accelerated towards the collector, the solvent evaporated, leaving only ultrathin fibers on the collector. The

obtained fibers were left exposed to ambient moisture (ca. 75% relative humidity) for approximately 12 h to allow complete hydrolysis of TTIP and consequently subjected to calcination at a high temperature ranging between 500 and 800 °C for 3 h, using the heating rate of 10 °C/min, both to remove the organic PVP and to allow for the formation of titania crystalline structures.

Morphology and size of the as-prepared titania fibers were observed by a JEOL JSM 5800 scanning electron microscope (SEM) and a JEOL JEM 2100 transmission electron microscope (TEM). The crystalline phase of the fibrous titania structures was studied at ambient condition with a Siemens D5000 X-ray diffractometer using  $\text{CuK}\alpha$  radiation and a Raman scattering microscope (BRUKER EQUINOX 55 FRA 106/5), after which the fraction of rutile in the product was calculated [15]. A thermogravimetric/differential thermal analyzer (TG/DTA, PERKIN-ELMER DIAMOND), operated at the heating rate of 10 °C/min under constant flow of air at 100 mL/min, was used to determine thermal decomposition behavior of the as-spun PVP/titania composite fibers. Lastly, the optical property of the composite fibers was investigated using a UV-visible scanning spectrophotometer (SHIMADZU UV-2550).

## 3. Results and discussion

### 3.1. Properties of as-spun fibers

Electrospinning of the prepared solution resulted in the ejection of the jet of the solution and the deposition of ultrathin fibers as a non-woven mat on the collector plate. Upon exposure to the ambient moisture, hydrolysis and subsequent condensation of TTIP within the fibers took place, resulting in the formation of Al-doped PVP/titania composite fibers. The XRD analysis revealed amorphous nature of the as-spun fibers (results not shown). According to SEM micrographs (Fig. 1), the fibers had smooth surface, with diameters in the range of 100–200 nm. It was also found that the content of aluminium nitrate within the spinning solution affected the obtained fibers in both the size and its distribution. As shown in Fig. 2, the increased amount of aluminium nitrate led to fibers with larger diameters. The average diameter of the as-spun fibers increased from 122 to 133, 149 and 184 nm when the aluminium nitrate content in the spinning solution was 0.1, 0.3 and 0.5 wt.%, respectively. It should be noted that the fiber diameters were measured by a SEM digital image analysis program (JEOL SemAfore 4.0). The average diameter was calculated from 50 fibers randomly selected from several locations in a sample. Three undoped samples were also employed to verify reproducibility of the data. The error bars in the figure represent standard deviation of the fiber diameter data. It can be observed that the distribution in the size of the fibers became increasingly broader as the aluminium nitrate content increased. This should be contributed to the increase in viscosity of the spinning solution, which led to non-uniform ejection of the jet [10].

To elucidate the effect of Al-doping on the properties of the spinning solution further, FT-IR analysis was conducted on the solutions that had been aged for various periods of time. The results for the neat spinning solution and the one doped with

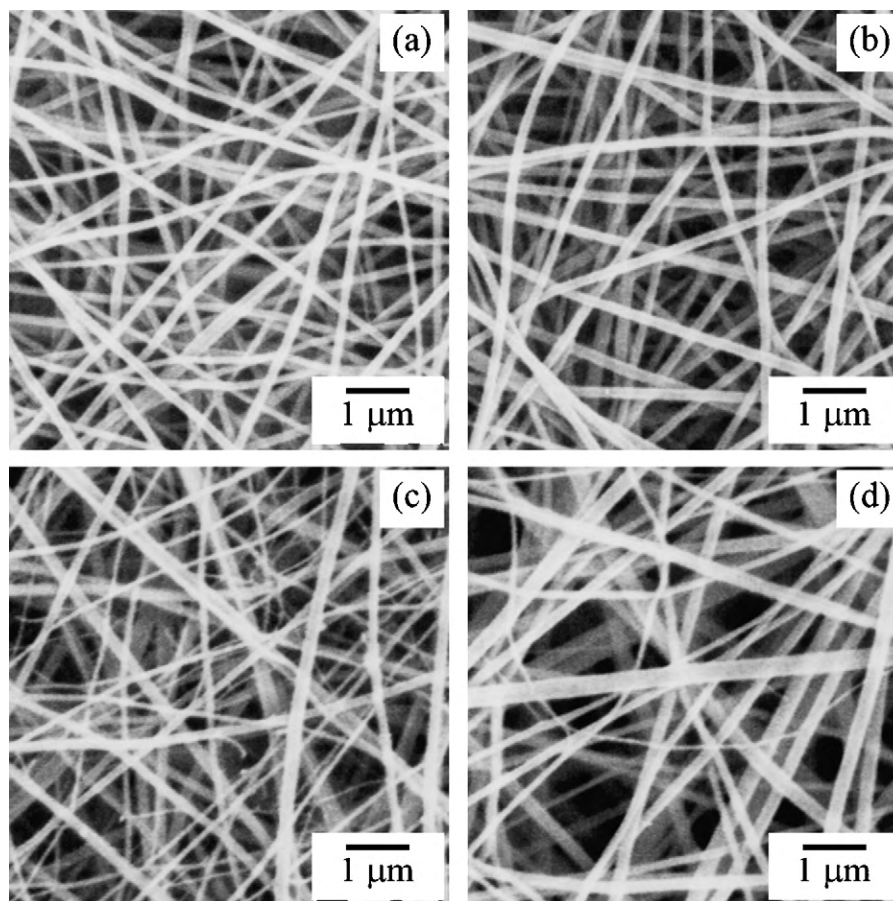


Fig. 1. SEM micrographs of as-spun fibers obtained from (a) neat PVP/TTIP spinning solution and the spinning solutions that contained aluminium nitrate in the amount of (b) 0.1 wt.%, (c) 0.3 wt.% and (d) 0.5 wt.%.

0.5 wt.% aluminium nitrate are shown in Fig. 3, in which the main absorption bands at 1375, 1090, 1045 and  $880\text{ cm}^{-1}$  are corresponding to ethanol [16]. The bands at 1715 and  $1666\text{ cm}^{-1}$  could be assigned to the carbonyl group of acetic acid [17] and the carbonyl stretching vibration of amide group of PVP [18], respectively. Upon the exposure to ethanol, the isopropoxy groups of TTIP were changed into ethoxy groups, as evidenced from the absorption bands at 1125 and  $930\text{ cm}^{-1}$

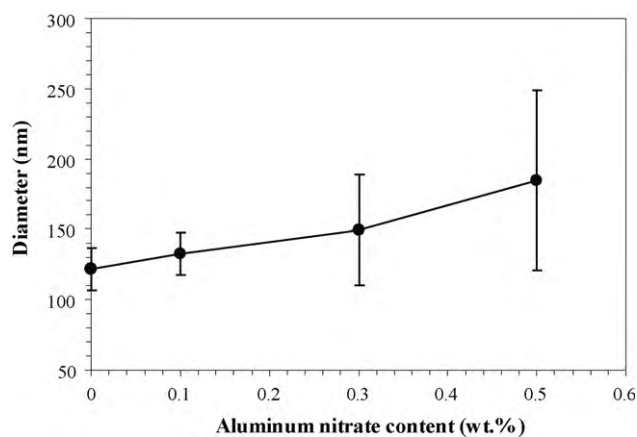


Fig. 2. Diameters of the as-spun fibers, as shown in Fig. 1, as a function of the aluminium nitrate content within the spinning solutions.

[16]. During aging, as the hydrolysis/condensation progressed, the intensity of the signal associated with the ethoxy groups decreased (owing to the formation of the Ti–O–Ti network). However, in the present work, the hydrolysis of titanium alkoxides was retarded by the chelating effect from acetic acid.

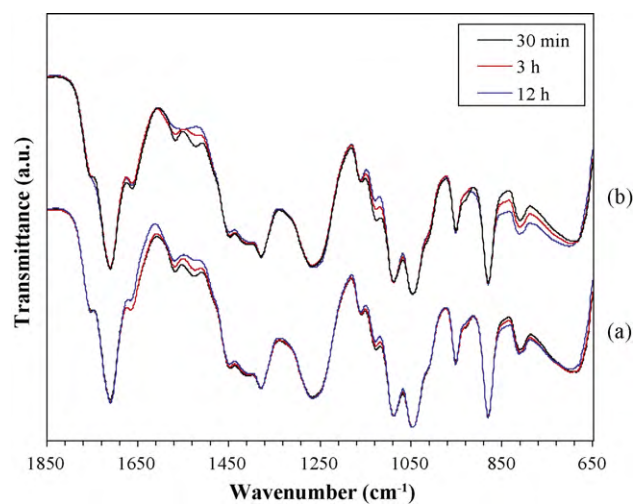


Fig. 3. FT-IR spectra of (a) the neat spinning solution and (b) the solution that contained 0.5 wt.% aluminium nitrate after having been aged for various periods of time.

The COO stretching vibration bands at 1521 and 1458  $\text{cm}^{-1}$  for the bidentate ligand, 1560 and 1419  $\text{cm}^{-1}$  for the bridging ligand, and 1276  $\text{cm}^{-1}$  for the monodentate ligand [19] were clearly visible. The intensities of these bands, especially those associated to the bidentate chelating effect, decreased as the condensation reaction progressed for longer aging periods.

For the spinning solution containing 0.5 wt.% aluminium nitrate, the intensity of the signal associated with the COO bidentate chelating effect decreased much quicker than that of the neat solution, while that of the band associated with the bridging ligand became broader. After 12 h of aging, only a broad band corresponding to the COO bridging was observed. The intensity of the signal associated with the ethoxy groups decreased significantly as well. All these results suggested that the addition of aluminium nitrate in the TTIP solution accelerated the condensation of the titanium oxide species, which was consistent with the dramatic increase in the viscosity of the aluminium nitrate-doped solutions as the aging period increased.

### 3.2. Properties of calcined fibers

As the electrospun fibers were subjected to calcination, the residual solvent and PVP matrix were removed from the fibers, while titania crystallized. Although both anatase and rutile phases were found in most calcined samples, it has been generally accepted that the rutile phase transformed from the anatase phase. For the fibers that were obtained from the neat TTIP solution, a substantial fraction of rutile was observed, even at a low calcination temperature of 500 °C. The higher the calcination temperature was, the greater the fraction of rutile

Table 1

Physical properties of neat and Al-doped titania fibers obtained after calcination at different temperatures.

Content of aluminium nitrate (wt.%)	Calcination temperature (°C)	Fraction of anatase phase (%)	Crystallite size (nm)	
			Anatase	Rutile
0 (undoped)	Pre-calcined	–	–	–
	500	67.3	20	23
	600	56.8	28	47
	700	9.8	34	87
	800	0	–	111
0.1	Pre-calcined	–	–	–
	500	95.2	15	17
	600	89.9	18	21
	700	47.1	27	38
	800	1.5	39	53
0.3	Pre-calcined	–	–	–
	500	100	11	–
	600	88.4	13	13
	700	80.5	18	16
	800	30.2	37	71
0.5	Pre-calcined	–	–	–
	500	100	10	–
	600	100	10	–
	700	95.4	17	15
	800	68.4	38	55

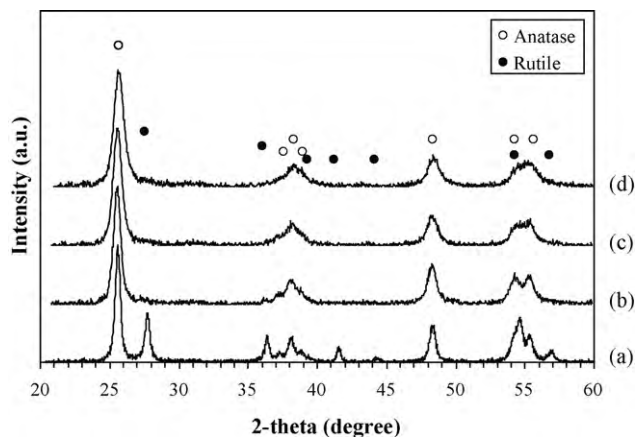


Fig. 4. XRD patterns of (a) neat titania fibers and the ones that were doped with (b) 0.1 wt.%, (c) 0.3 wt.% and (d) 0.5 wt.% aluminium nitrate, after having been calcined at 500 °C for 3 h.

phase was. Titania in rutile phase, with undetectable fraction of anatase, was obtained after the fibers had been calcined at 800 °C (see Table 1). On the other hand, when the spinning solution was doped with aluminium nitrate, the calcined fibers contained greater fractions of anatase phase, as compared to the fibers obtained from the neat spinning solution. This is evident from the XRD patterns of these products in Fig. 4. It should be noted that no XRD patterns associated with neither aluminium oxide nor aluminium titanate were observed in all samples, indicating that Al was incorporated well into the lattice of titania rather than just forming as an oxide layer on the surface of titania crystallites [20]. These behaviors were also observed from Raman spectra of the calcined products in Fig. 5. After having been calcined at 800 °C for 3 h, the neat titania fibers exhibited overwhelming signals at 244, 450 and 611  $\text{cm}^{-1}$ , corresponding to rutile phase [21], while anatase was still present in significant fraction in the Al-doped fibers, especially ones doped with 0.5 wt.% aluminium nitrate, as witnessed from the signals at 141, 193, 394, 520 and 636  $\text{cm}^{-1}$  [21]. The results from the analysis with Raman spectroscopy not only concurred with the XRD analysis in the regard of anatase-rutile phase

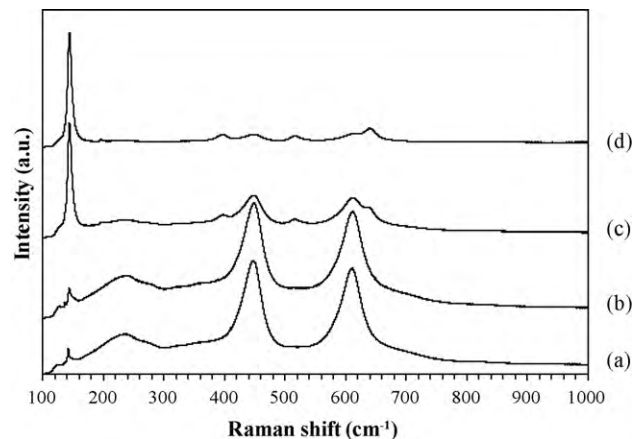


Fig. 5. Raman spectra of (a) neat titania fibers and the ones that were doped with (b) 0.1 wt.%, (c) 0.3 wt.% and (d) 0.5 wt.% aluminium nitrate, after having been calcined at 800 °C for 3 h.



transformation, but they also confirmed that aluminium oxide was not formed in Al-doped products. No signal from other compound, besides those from titania, was detected in all samples. Nevertheless, the presence of aluminium in the calcined samples was confirmed by the analysis via the energy dispersive X-ray spectroscopy (EDX) equipped on the SEM. According to the EDX measurement, the aluminium content of the calcined fibers prepared with 0.3 and 0.5 wt.% aluminium nitrate was found to be 0.55 and 0.88 wt.%, respectively. For the fibers with 0.1 wt.% aluminium nitrate, however, the Al content was too low to be detectable by EDX.

By incorporating Al into titania, the temperature at which the rutile phase was predominant also increased dramatically. In other words, thermal stability of the anatase phase was enhanced by the presence of Al. This retardation effect towards the phase transformation from anatase to rutile of titania agreed well with a previous report by Yang et al. [20]. This effect became more apparent as the Al content was increased. According to the DTA results in air (i.e., an attempt to simulate the calcination of the fibers) in Fig. 6, the undoped fibers exhibited exothermic peaks at 335, 460 and 490 °C, corresponding to the thermal decomposition of PVP, crystallization of amorphous titania into anatase phase, and subsequent phase transformation from anatase to rutile, respectively [22]. For the Al-doped fibers, an additional peak at 240 °C, associated with the thermal decomposition of

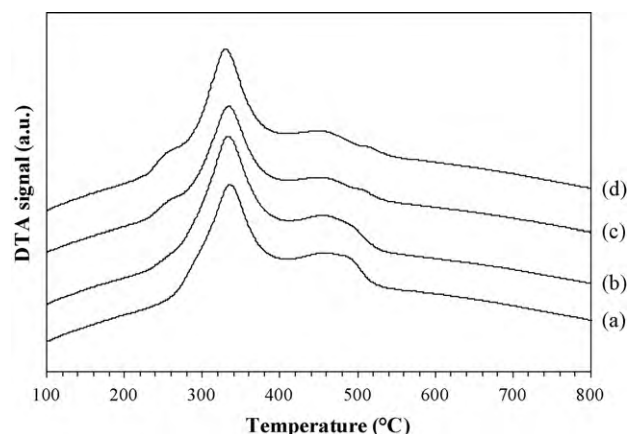


Fig. 6. DTA curves of as-spun fibers obtained from (a) neat spinning solution and the spinning solutions that contained aluminium nitrate in the amount of (b) 0.1 wt.%, (c) 0.3 wt.% and (d) 0.5 wt.%.

nitrate group, was observed. More importantly, the temperature at which the anatase-to-rutile phase transformation occurred shifted towards a higher temperature as the Al content increased, i.e., from 490 to 515 °C when the Al content increased from 0 to 0.5 wt.%. On the other hand, the temperature at which the amorphous-to-anatase phase transformation occurred was unaffected. This is in contrast with the report by Kim et al.

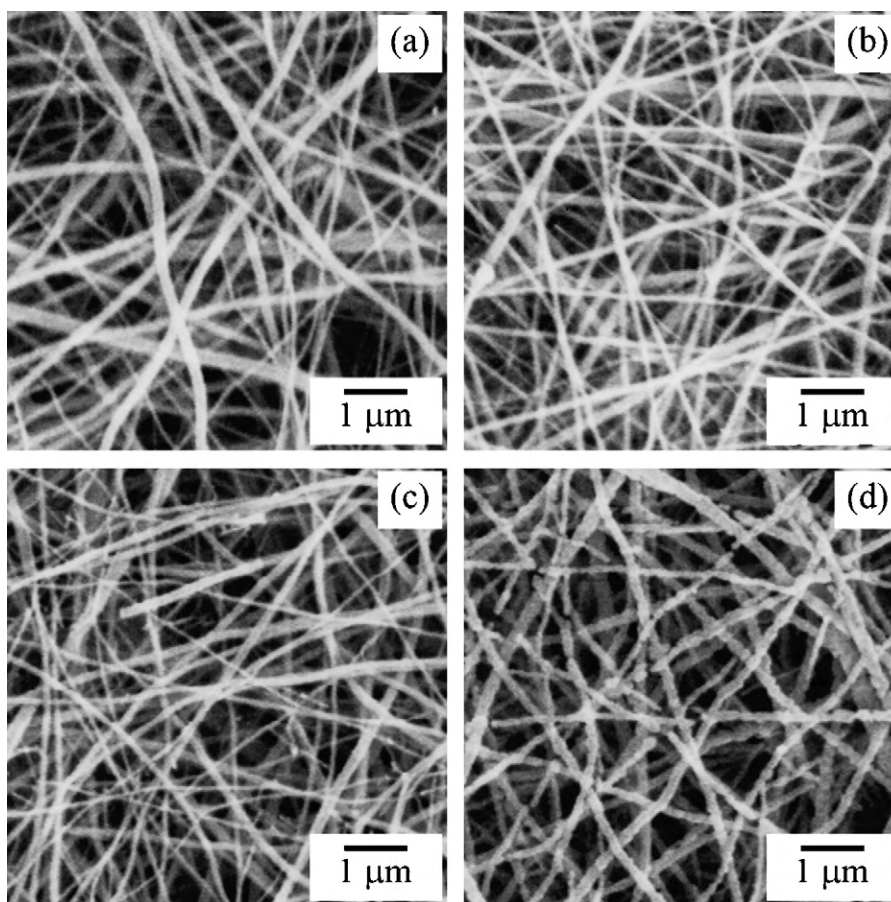


Fig. 7. SEM micrographs of fibers prepared from the spinning solution containing 0.5 wt.% aluminium nitrate, after having been calcined at (a) 500 °C, (b) 600 °C, (c) 700 °C and (d) 800 °C for 3 h.

[13] in that Al dopant retarded both the amorphous-to-anatase and the anatase-to-rutile phase transformations.

Table 1 also shows crystallite sizes of both anatase and rutile phases within the fibers. These were calculated from the well-known Scherrer equation based on (1 0 1) scattering plane of anatase and (1 1 0) plane of rutile, respectively. The crystallite size of the anatase phase in the undoped fibers increased steadily with an increase in the calcination temperature. The same trend was also observed with that of the rutile phase, but in a much greater extent. The incorporation of Al in the lattices of titania in both anatase and rutile crystallographic forms suppressed the growth of the corresponding crystallites effectively, especially at relatively low calcination temperatures. This was a result of the fact that Al can reduce the sintering rate [13]. This accordingly affected the surface morphology of the calcined fibers. It was obvious from SEM micrographs shown in Fig. 7 that the surface of the fibers became rougher as the calcination temperature increased. There was also evidence for fibers breaking up into shorter pieces due to the shrinkage caused mainly by the removal of the PVP matrix from the fibers during the calcination. The removal of PVP also caused the reduction in diameters of the fibers, as summarized in Fig. 8. Nevertheless, the size of the Al-doped fibers was still larger than that of the undoped ones, because of the larger size of the fibers as-spun from the aluminium nitrate-doped solutions mentioned earlier. It should be noted that the calcination was conducted at 500, 600, 700 and 800 °C, respectively. Some data points in Fig. 8 were intentionally shifted in the X-direction for clarity and the error bars represent the standard deviation of the data.

Further investigation using TEM equipped with the selected area electron diffraction (SAED) revealed the polycrystalline nature of the calcined fibers (Fig. 9). The individual fiber consisted of nanosized crystalline domains, each of which was suggested to be titania single crystal according to the interference pattern observed from high resolution TEM images and a good agreement between the domain sizes as observed by TEM and the crystallite sizes of

titania as calculated from the XRD line broadening. Comparison of the TEM images between Fig. 9a and b revealed that the Al-doped fiber consisted of a great number of densely packed crystallites, while those of the undoped fiber were much larger. This could be a result of the increase in the nucleation rate of titanium oxide seeds induced by the presence of Al, during the sol–gel condensation process, as previously observed by the FT-IR analysis of the spinning solution. These seeds were subsequently converted to titania in anatase and rutile phases during the calcination, hence the greater number of titania crystallites as observed in Fig. 9b. It should also be noted that Al-doping not only affected the size and number of the crystallites constituting the fibers, but it affected the shape of the crystallites as well. The Al-doped crystallites appeared to be more spherical in shape than the undoped counterparts. This result suggested that Al also played a major role in controlling the growth mechanism of the titania crystallites.

The optical property of the products was observed with the UV-visible scanning spectrophotometer. The UV/Vis spectra of the calcined titania fibers synthesized with different amounts of Al dopant are shown in Fig. 10. A slight shift of the band edge towards the visible region was observed for the Al-doped titania fibers, which suggested the narrowing of the band gap due to the interstitial Al species within the titania crystal structures [12].

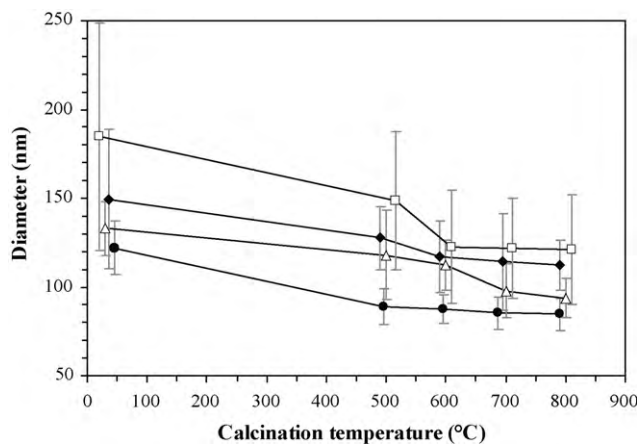


Fig. 8. Diameters of (●) the neat titania fibers and the titania fibers obtained from the spinning solutions containing (△) 0.1 wt.%, (◆) 0.3 wt.% and (□) 0.5 wt.% aluminium nitrate as a function of the calcination temperature.

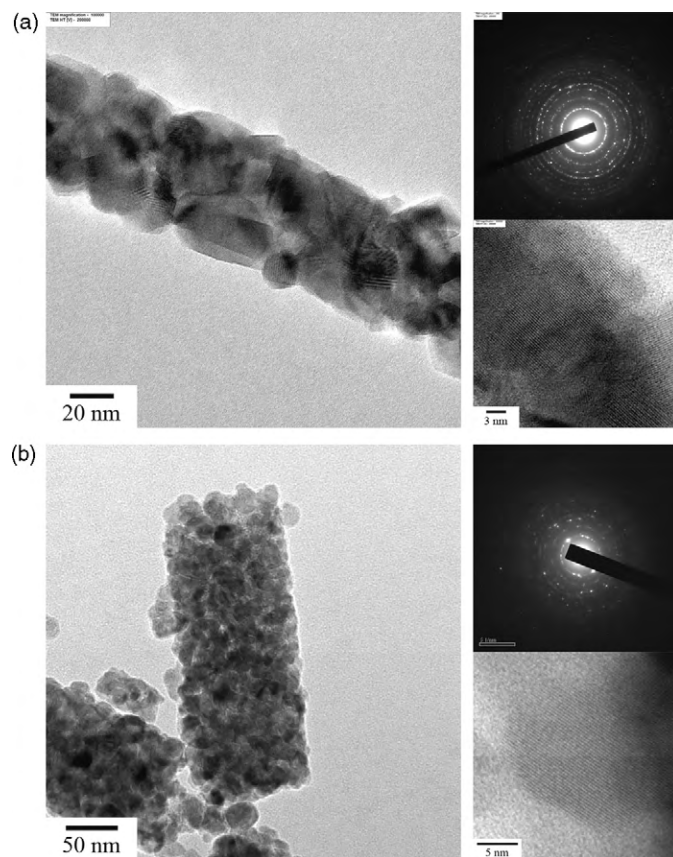


Fig. 9. TEM micrographs and corresponding SAED patterns of (a) a piece of the neat titania fiber and (b) a piece of the Al-doped titania fiber obtained from the spinning solution containing 0.5 wt.% aluminium nitrate, after having been calcined at 500 °C for 3 h.

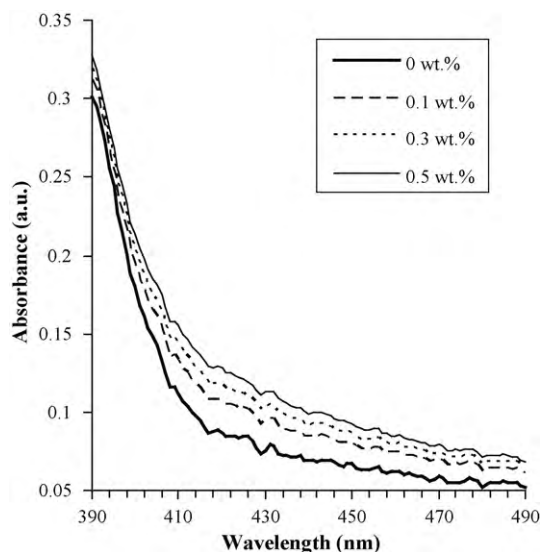


Fig. 10. UV–visible spectra of the neat titania fibers and the titania fibers obtained from the spinning solutions containing 0.1, 0.3 and 0.5 wt.% aluminium nitrate, after having calcined at 500 °C for 3 h.

The extent of the shift increased obviously with an increase in the amount of Al dopant.

#### 4. Conclusions

In the present contribution, neat and aluminium-doped titanium (IV) oxide fibers were successfully prepared by combined sol–gel and electrospinning techniques. These fibers were obtained after calcination of the as-spun polyvinylpyrrolidone (PVP)/titania composite fibers, with or without aluminium nitrate, at temperatures in the range of 500–800 °C. The products were round fibers with smooth surfaces. The addition of aluminium nitrate in the spinning solution accelerated condensation of the titanium oxide species, which dramatically increased the viscosity of the Al-doped solution and consequently affected the average diameters, as well as distribution of diameters, of the as-spun fibers. The aluminium dopant also played the major roles in both regulating the nucleation rate of titanium oxide seeds during crystallization as well as controlling the growth mechanism of the titania crystallites. In addition, the presence of aluminium dopant significantly improved thermal stability of anatase phase, i.e., retarded anatase-to-rutile phase transformation, within the obtained titania fibers. Specifically, the titania fibers doped with 0.5 wt.% aluminium nitrate still contained the anatase phase of about 68% after being calcined at 800 °C, while the neat titania fibers calcined at the same condition were pure rutile.

#### Acknowledgements

This research was supported in part by a grant under the Strategic Scholarships for Frontier Research Network for the Thai Doctoral Degree Program from the Office of the Higher Education Commission, Ministry of Education, Thailand.

#### References

- [1] D. Li, Y.N. Xia, Fabrication of titania nanofibers by electrospinning, *Nano Lett.* 3 (4) (2003) 555–560.
- [2] P. Viswanathamurthi, N. Bhattarai, C.K. Kim, H.Y. Kim, D.R. Lee, Ruthenium doped TiO<sub>2</sub> fibers by electrospinning, *Inorg. Chem. Commun.* 7 (5) (2004) 679–682.
- [3] J. Klongdee, W. Petchkroh, K. Phuempoonsathaporn, P. Praserttham, A.S. Vangnai, V. Pavarajarn, Activity of nanosized titania synthesized from thermal decomposition of titanium (IV) *n*-butoxide for the photocatalytic degradation of diuron, *Sci. Technol. Adv. Mater.* 6 (3–4) (2005) 290–295.
- [4] C.H. Kwon, H.M. Shin, J.H. Kim, W.S. Choi, K.H. Yoon, Degradation of methylene blue via photocatalysis of titanium dioxide, *Mater. Chem. Phys.* 86 (1) (2004) 78–82.
- [5] S.J. Kim, S.D. Park, Y.H. Jeong, S. Park, Homogeneous precipitation of TiO<sub>2</sub> ultrafine powders from aqueous TiOCl<sub>2</sub> solution, *J. Am. Ceram. Soc.* 82 (4) (1999) 927–932.
- [6] Z. Ding, X.J. Hu, G.Q. Lu, P.L. Yue, P.F. Greenfield, Novel silica gel supported TiO<sub>2</sub> photocatalyst synthesized by CVD method, *Langmuir* 16 (15) (2000) 6216–6222.
- [7] J. Yang, S. Mei, J.M.F. Ferreira, Hydrothermal synthesis of nanosized titania powders: influence of tetraalkyl ammonium hydroxides on particle characteristics, *J. Am. Ceram. Soc.* 84 (8) (2001) 1696–1702.
- [8] S. Iwamoto, W. Tanakulrungsank, M. Inoue, K. Kagawa, P. Praserttham, Synthesis of large-surface area silica-modified titania ultrafine particles by the glycothermal method, *J. Mater. Sci. Lett.* 19 (16) (2000) 1439–1443.
- [9] K.Y. Jung, S.B. Park, Enhanced photoactivity of silica-embedded titania particles prepared by sol–gel process for the decomposition of trichloroethylene, *Appl. Catal. B: Environ.* 25 (4) (2000) 249–256.
- [10] C. Mit-upphatham, M. Nithitanakul, P. Supaphol, Ultrafine electrospun polyamide-6 fibers: effect of solution conditions on morphology and average fiber diameter, *Macromol. Chem. Phys.* 205 (17) (2004) 2327–2338.
- [11] K.Y. Jung, S.B. Park, Anatase-phase titania: preparation by embedding silica and photocatalytic activity for the decomposition of trichloroethylene, *J. Photochem. Photobiol. A: Chem.* 127 (1–3) (1999) 117–122.
- [12] J.E. Lee, S.M. Oh, D.W. Park, Synthesis of nano-sized Al doped TiO<sub>2</sub> powders using thermal plasma, *Thin Solid Films* 457 (1) (2004) 230–234.
- [13] J. Kim, K.C. Song, S. Foncillas, S.E. Pratsinis, Dopants for synthesis of stable bimodally porous titania, *J. Eur. Ceram. Soc.* 21 (16) (2001) 2863–2872.
- [14] M. Hirano, K. Ota, Direct formation and photocatalytic performance of anatase (TiO<sub>2</sub>)/silica (SiO<sub>2</sub>) composite nanoparticles, *J. Am. Ceram. Soc.* 87 (8) (2004) 1567–1570.
- [15] X.Z. Fu, L.A. Clark, Q. Yang, M.A. Anderson, Enhanced photocatalytic performance of titania-based binary metal oxides: TiO<sub>2</sub>/SiO<sub>2</sub> and TiO<sub>2</sub>/ZrO<sub>2</sub>, *Environ. Sci. Technol.* 30 (2) (1996) 647–653.
- [16] M. Burgos, M. Langlet, The sol–gel transformation of TIPT coatings: a FTIR study, *Thin Solid Films* 349 (1–2) (1999) 19–23.
- [17] R.H. Sui, A.S. Rizkalla, P.A. Charpentier, FTIR study on the formation of TiO<sub>2</sub> nanostructures in supercritical CO<sub>2</sub>, *J. Phys. Chem. B* 110 (33) (2006) 16212–16218.
- [18] M.F. Silva, C.A. da Silva, F.C. Fogo, E.A.G. Pineda, A.A.W. Hechenleitner, Thermal and FTIR study of polyvinylpyrrolidone/lignin blends, *J. Therm. Anal. Calorim.* 79 (2) (2005) 367–370.
- [19] H.J. Chen, P.C. Jian, J.H. Chen, L. Wang, W.Y. Chiu, Nanosized-hybrid colloids of poly(acrylic acid)/titania prepared via in situ sol–gel reaction, *Ceram. Int.* 33 (4) (2007) 643–653.
- [20] J. Yang, Y.X. Huang, J.M.F. Ferreira, Inhibitory effect of alumina additive on the titania phase transformation of a sol–gel-derived powder, *J. Mater. Sci. Lett.* 16 (23) (1997) 1933–1935.
- [21] Y. Djaoued, S. Badilescu, P.V. Ashrit, D. Bersani, P.P. Lottici, J. Robichaud, Study of anatase to rutile phase transition in nanocrystalline titania films, *J. Sol–Gel Sci. Technol.* 24 (2002) 255–264.
- [22] S.S. Hong, M.S. Lee, S.S. Park, G.D. Lee, Synthesis of nanosized TiO<sub>2</sub>/SiO<sub>2</sub> particles in the microemulsion and their photocatalytic activity on the decomposition of *p*-nitrophenol, *Catal. Today* 87 (1–4) (2003) 99–105.